Liquid Crystal-Based Surface Plasmon Resonance Biosensor

Ali Vahedi [1,2] · Mohammad Kouhi [1,2]

Abstract

Surface plasmon resonance has many applications in designing biosensors. In this paper, an easy fabrication liquid crystal-based surface plasmon resonance (LC-SPR) biosensor is simulated and presented which can determine reflectance and sensitivity via liquid crystal structure, gold structure, and silver structure. The powerful transfer matrix was applied for calculating the reflectance and sensitivity of the biosensor. The alignment of liquid crystal molecules and the concentration of biological analytes have a remarkable impact on biosensor's sensitivity enhancement. The results indicated that, after including analytes, the birefringence of liquid crystal changes; consequently, performance parameters are enhanced. Maximum performance parameters of the proposed LC-SPR biosensor obtained for the homogeneous condition of $S = 0$ and silver-based structure parameters are better than those of other structures.

Keywords Biosensors · Liquid crystals · Surface plasmon resonance · Birefringence

Introduction

Due to their unique electro-optical properties, liquid crystals (LCs) have several applications in LCD devices, optical materials, chemicals, and biological fields [1–5]. Many research studies have been conducted on biosensing applications of liquid crystals. The combination of LCs with sensing systems and the detection of significant optical effects which allow for quick response imagining make it possible to use LCs in sensing applications. For instance, nematic LCs are very useful in detecting biomolecules [6, 7], polymer chemicals, and heavy metal ions [8]. In recent years, a significant variety of research studies including electrochemical, bioelectronic, cellular and molecular identification, piezoelectric, and some optical biosensors have been dedicated to biosensing [3, 7–10]. In these sensors, the orientation of LC molecules changes, and thin films are influenced by external factors. Due to the collective behavior of the LC molecules, a change in the direction of molecules by the surface, biological, or chemical elements leads to a change in the whole of the structure [9]. For example, in reference [8], the substrate has been aligned homeotropically with 4-pentyl-4-cyanobiphenyl (5CB) liquid crystal, under the influence of dimethyl methyl phosphonate (DMMP) solution, 5CB molecules can be rotated; then these alerts related to concentration of the solution. The rotation of 5CB molecules is considered as alerts of solution concentration. Some biosensors are capable of detecting and analyzing structures by using transmitted light of an optical sample. These transductions include optical microscopes and surface plasmon resonance (SPR) [2, 9]. Optical microscope indicates the deformation of LC identification by using light polarization which passes through anisotropic material [10–12]. Surface plasmon wave was firstly used in 1968 by Kretschmann and Otto via attenuated total reflection method [13]. In the past two decades, SPR has played a promising role in many biological and chemical sensing applications [14]. Some researchers used SPR phenomenon-based methods in the metal/dielectric interface. LC is used as a dielectric material for detecting biological agents [15–18]. LC-based SPR biosensors are superior to conventional SPRs which are made of isotropic materials [19]. For example, an optical fiber SPR sensor filled with LC may be used as a thermometer and has more than 46-nm wavelength shifts, which is due to phase transition between nematic and isotropic phases [20]. Another merit of LC-based SPR biosensors is that transition from the nematic phase to the isotropic phase, due to increased temperature, is sensitive to small changes in the density of the analyte [21]. Hence, it can be argued that the application of optical-transmission LC-SPR biosensors offers many significant advantages. As a result, a

✉ Ali Vahedi
vahedi@iaut.ac.ir

1 Department of Physics, Tabriz Branch, Islamic Azad University, Tabriz, Iran

2 Biophotonic Research Center, Tabriz Branch, Islamic Azad University, Tabriz, Iran

Fig. 1 Schematic of LC-SPR biosensor: **a** homeotropically aligned LC molecules in the absence of biological agents; **b** LC film alignment will deform in the presence of biological agents
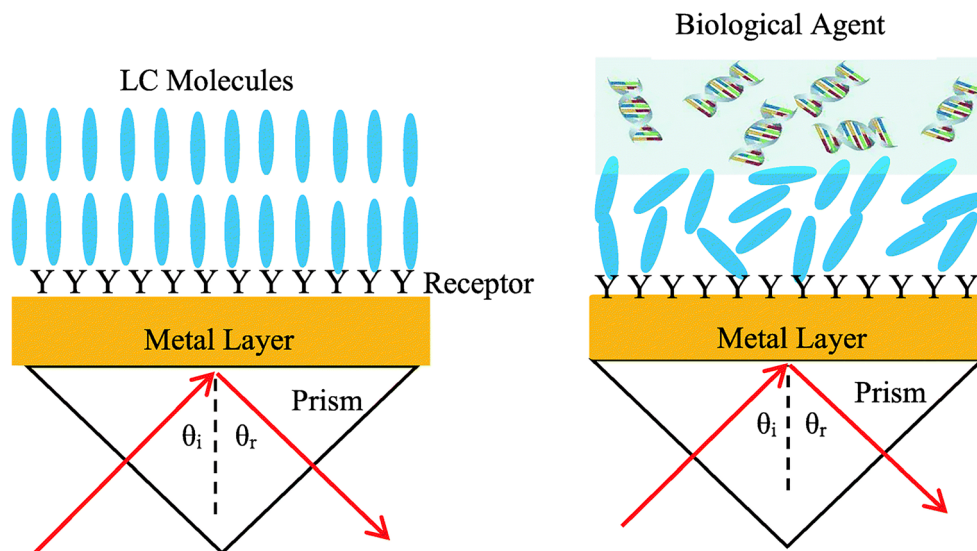

simpler system with a low error probability provides the opportunity for the detecting and tracking order parameter. The alignment of LC molecules in the anisotropic phase makes the molecular LC film orientation possible for partial and complete ordering. This approach can potentially detect and track changes in the texture and order parameters of the LC [9].

In this article, we used LC-SPR biosensor in which 5CB nematic liquid crystal was considered as the dielectric sensitive layer. At first, all 5CB molecules had homogeneous or homeotropic alignment on the metal layer. When the analyte was added to LC, 5CB molecules and analytes stuck together and changed the orientation of the director axis. Biosensor reflectivity and sensitivity were simulated with regard to several concentrations of analytes or several LC birefringences.

General Principle of LC-SPR Biosensor

The proposed LC-SPR sensor based on metal/liquid crystal structure is shown in Fig. 1. It consists of three different layers.
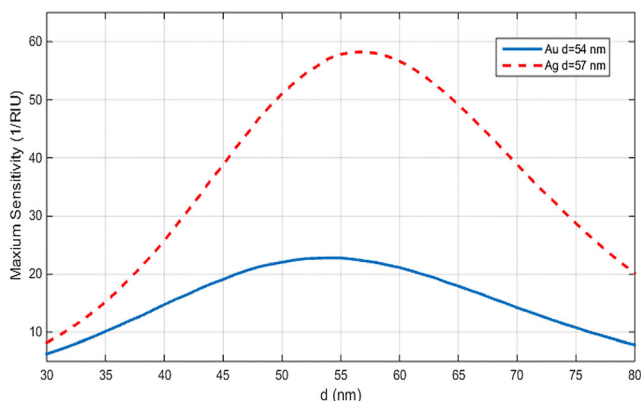
Fig. 2 Maximum sensitivity of LC-SPR biosensor versus gold (silver) film thickness

The first layer is a high-refractive index prism and the second layer is a thin gold or silver film. Thanks to their excellent optical specifications, gold and silver are regarded as standard materials for SPR sensors. The third layer is a sensing layer which includes liquid crystal and biological or chemical agents.

Although some surface pre-partitions are experimentally required for immobilizing LC and biological agents on silver or gold, a simple three-layer model (glass layer, metal layer, and sensing layer) was used without modeling the pre-partition layer in this simulation. When compared with the impacts of other layers, the effect of the preparation layer could be ignored because it has a low refractive index and ultra-thin thickness [22]. Stability of this biosensor is dependent on the stability of the immobilized biological agents and liquid crystal alignments quality.

Now, the modeling used for computing reflectivity and sensitivity of LC-SPR biosensors is discussed and described. As shown in Fig. 1, in Kretschmann configuration, SPR sensor with TM-polarized laser light incidents is on one lateral face of the prism; as a result, a total reflection phenomenon occurs. The attenuated wave passes through a metal and upper dielectric interface; then, a wave vector of the incident light matches the wave vector of the SP wave. The SP resonantly couples with the incident light and a great electric field is sensed; the so-called SP resonance (SPR) occurs [23].

Theory

The proposed LC-SPR sensor consists of three different layers. The first layer is the prism for exciting SP waves; the second layer is the metal layer and the third layer is liquid crystal sensing medium. The high index prism (LASF35) has a refractive index of $n_1 = 2.01493$ at 633 nm [9]. Au (Ag) is regarded as the metal thin film with an optimal

Fig. 3 Reflection spectrums in homeotropic alignment ($\theta_d = 0^o$) of the 5CB molecule with gold metal layer. **a** Different degrees of ordering; **b** various concentrations of the biological agent (Δn) in $S = 1$
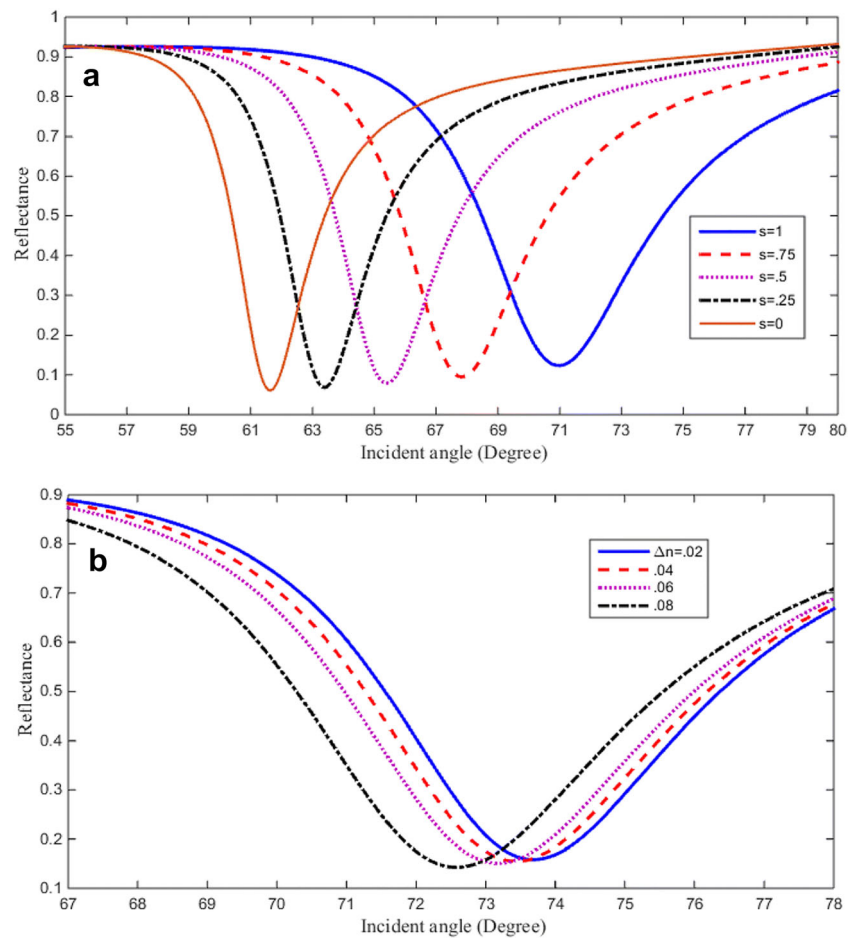
thickness, and its dielectric constant is determined through the Drude-Lorentz model in the following:

$$\varepsilon_m = 1 - \frac{\lambda^2 \lambda_c}{\lambda_p^2 (\lambda_c + i\lambda)} \tag{1}$$

In this formula, $\lambda_{pAu} = 0.16826$ μm ($\lambda_{pAg} = 0.14541$ μm) and $\lambda_{cAu} = 8.9342$ μm ($\lambda_{cAg} = 17.614$ μm) indicate the plasma and collision wavelengths of Au (Ag) respectively [22]. The liquid crystal layer, as the last layer, should be described more precisely because it is an anisotropic material.

Since nematic LCs are mostly known as diamagnetic materials, their relative permeability is close to unity. In general, the electric permittivity for the incompletely ordered LC layer is a tensor. The dielectric tensor of the anisotropic liquid crystal layer in the coordinate system can be shown as follows [24]:

$$\overline{\varepsilon} = \begin{bmatrix} \varepsilon_{xx} & \varepsilon_{yy} & \varepsilon_{xz} \\ \varepsilon_{yx} & \varepsilon_{yy} & \varepsilon_{yz} \\ \varepsilon_{zx} & \varepsilon_{zy} & \varepsilon_{zz} \end{bmatrix} \tag{2}$$

where ε_{ij} denotes the dielectric constant induced by the electric field in the ij direction. For the partially ordered LC

in which the director makes the φ angle with respect to the z-axis and where metal interface layer is on the x-axis, the dielectric tensor can be written as follows:

$$\overline{\varepsilon} = \begin{bmatrix} \varepsilon_{xx} & 0 & \varepsilon_{xz} \\ 0 & \varepsilon_{yy} & 0 \\ \varepsilon_{zx} & 0 & \varepsilon_{zz} \end{bmatrix} \tag{3}$$

where:

$$\begin{aligned} \varepsilon_{xx} &= \varepsilon_{is} + S\Delta\varepsilon \left(\sin^2\varphi - \frac{1}{3} \right) \\ \varepsilon_{zz} &= \varepsilon_{is} + S\Delta\varepsilon \left(\cos^2\varphi - \frac{1}{3} \right) \\ \varepsilon_{xz} &= S\Delta\varepsilon \sin\varphi \cos\varphi \end{aligned} \tag{4}$$

In these relations, ε_{is} represents permittivity in the isotropic state which is specified by: $\varepsilon_{is} = (2\varepsilon_\parallel - \varepsilon_\perp)/3$ where $\varepsilon_\parallel$, $\varepsilon_\perp$ are ordinary and extraordinary dielectric constants at the completely ordered state. $\Delta\varepsilon = \varepsilon_\parallel - \varepsilon_\perp$ is labeled as LC dielectric anisotropy and S is the order parameter which can be summarized according to this mathematical description: $S = \frac{1}{2}$

Fig. 4 Sensitivity in homeotropic alignments ($\theta_d = 0^o$) of the 5CB molecule with the gold metal layer. **a** Different degrees of ordering; **b** sensitivity for various concentrations of the biological agent (Δn)
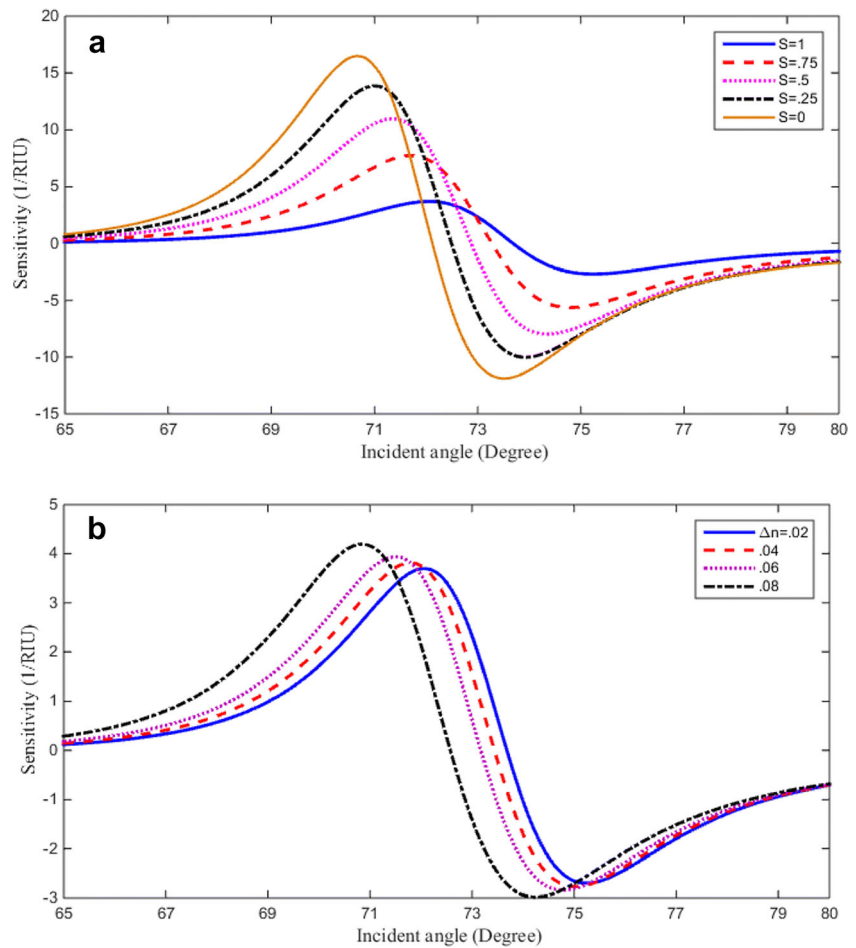
$< 3\cos^2\theta_d - 1 >$ where θ_d and $< >$ denote the angle between the long axis of the rod-like molecule with the director axis and statistical average, respectively [25].

The effective refractive index of the unstable evanescent wave in the LC layer is computed via Maxwell's equations and plane waves in the partially ordered uniaxial media [9, 26]:

$$n_{\text{eff}} = \left[\frac{\varepsilon_{os}\varepsilon_{es}}{\varepsilon_{os} + S\Delta\varepsilon(k.n)^2} \right]^{0.5} \tag{5}$$

where $\varepsilon_{os} = \varepsilon_{is} - S\frac{\Delta\varepsilon}{3}$ and $\varepsilon_{es} = \varepsilon_{is} + 2S\frac{\Delta\varepsilon}{3}$. In this equation, $k. n$, ε_{os}, and ε_{es} are demonstrated vectors in the direction of the refracted wave vector, director axis, ordinary, and extraordinary dielectric constants of LC, respectively.

Now, the N-layer modeling used for calculating LC-SPR biosensor reflectivity and sensitivity is discussed. Since the transfer matrix is a powerful and straightforward method for the N-layer, it was used in the proposed LC-SPR biosensor. In this structure, we have three layers which were considered along the z-axis. The dielectric constant and refractive index (RI) of the ith layer are denoted by ε_i and n_i, respectively. By applying the boundary condition, the tangential fields at layer

$N + 1$ are presented in terms of the tangential fields at N in the following way [23]:

$$\begin{bmatrix} E_{N+1} \\ H_{N+1} \end{bmatrix} = \begin{bmatrix} M_{11} & M_{12} \\ M_{21} & M_{22} \end{bmatrix} \begin{bmatrix} E_N \\ H_N \end{bmatrix} \tag{6}$$
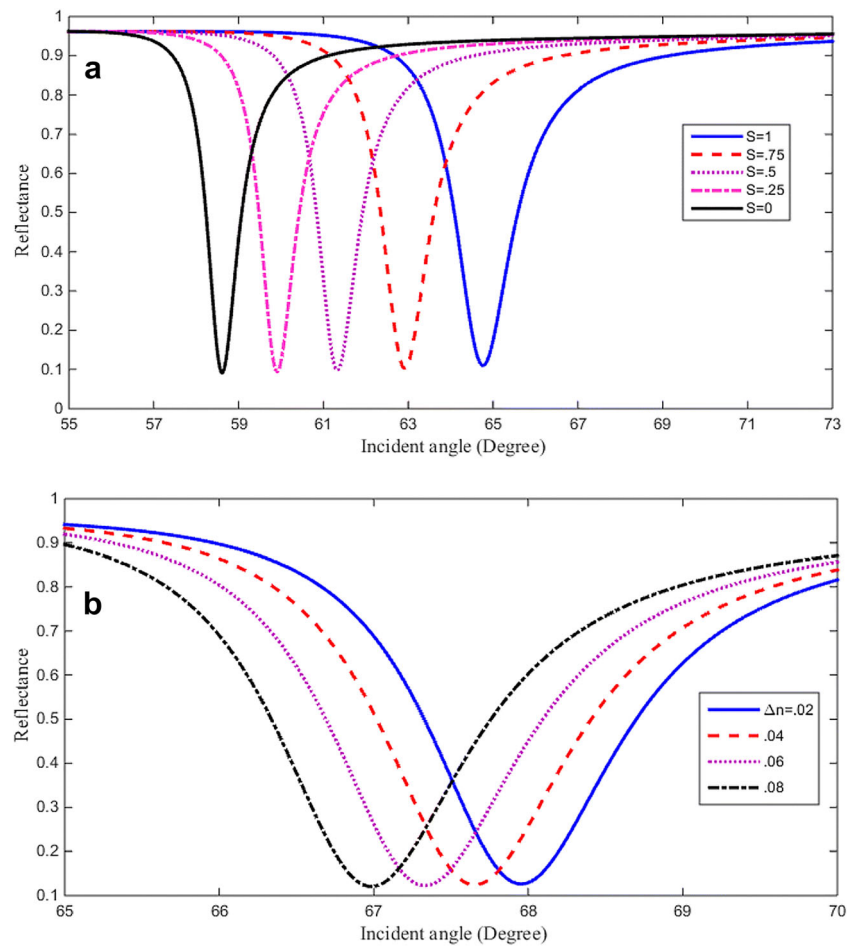
where E_N and H_N represent the tangential components of electric and magnetic fields at the boundary of the Nth layer; in a similar vein, E_{N+1} and H_{N+1} are the fields for the boundary at the $(N+1)$th layer. M_{ij} indicates the characteristics matrix of the Nth layer. For a combined structure with N layers, a total transition matrix is the product of all layer matrixes, and for the p-polarized light, it can be determined as follows:

$$M_{ij} = \left(\prod_{k=1}^{N} M_k \right) ij = \begin{bmatrix} M_{11} & M_{12} \\ M_{21} & M_{22} \end{bmatrix} \tag{7}$$

where:

$$M_K = \begin{bmatrix} \cos\beta_K & -i\sin\beta_k/q_k \\ -iq_K\sin\beta_k & \cos\beta_K \end{bmatrix} \tag{8}$$

Fig. 5 Reflection curves in homeotropic alignment ($\theta_d = 0^o$) of the 5CB molecule with the silver metal layer. **a** Different degrees of ordering; **b** reflection spectrums for various concentrations of the biological agent (Δn) in $S = 1$

$$q_k = \left(\frac{\mu_k}{\varepsilon_k}\right)^{\frac{1}{2}} \beta_k = \frac{2\pi n_k}{\lambda} \cos\theta_k (z_k - z_{k-1}) = \frac{2\pi d_k}{\lambda} \left(\varepsilon_k - n_1^2 \sin^2\theta_1\right)^{\frac{1}{2}} \quad (9)$$

$$\cos\theta_K = \frac{\left(\varepsilon_k - n_1^2 \sin^2\theta_1\right)^{\frac{1}{2}}}{\varepsilon_k}$$

Here, θ_1 and λ are the incident angle and wavelength. The amplitude of the reflection coefficient (rp) for the TM polarization light is obtained as follows:

$$r_p = \frac{(M_{11} + M_{12}q_N)q_1 - (M_{21} + M_{22}q_N)}{(M_{11} + M_{12}q_N)q_1 + (M_{21} + M_{22}q_N)} \quad (10)$$

Hence, the reflectance of the N-layer model for the TM-polarized light can be written as follows:

$$R = |r_p|^2 \quad (11)$$

Here, three performance parameters, namely sensitivity, detection accuracy, and quality factor are discussed. Sensitivity (S) is the ratio of change in resonance angle ($\Delta\theta_{res}$) to the change in birefringence of the sensing medium $\Delta(\Delta n_{eff})$. Δn_{eff} indicates effective birefringence of 5CB bounded by air and solution at different sodium dodecyl sulfate (SDS) concentrations [27, 28]. The resonance angle and Δn_{eff} are measured in the unit of degree and refractive index (RIU), respectively.

The change in SDS concentrations and biological agents ($\Delta(\Delta n_{eff})$) of the sensing medium would lead to a change in reflectance (R). A great change in R value leads to a high sensitivity. In correspondence with the change in the refractive index of the sensing medium, the reflectance change is regarded as dR; hence, sensitivity can be defined as follows:

$$S = \frac{\Delta\theta_{res}}{\Delta(\Delta n_{eff})} \cong \frac{d\theta}{d(\Delta n_{eff})} = \frac{d\theta}{dR} \times \frac{dR}{d(\Delta n_{eff})} \quad (12)$$

Quality factor (QF) is defined as the ratio of sensitivity to the full width at half maximum (FWHM) of the SPR curve, and detection accuracy (DA) is defined as the ratio of the shift in the resonance angle ($\Delta\theta_{res}$) to the FWHM of the reflectance curve [29].

$$QF = \frac{S}{FWHM} \quad (13)$$

$$DA = \frac{\Delta\theta_{res}}{FWHM} \quad (14)$$

Fig. 6 Sensitivity in homeotropic alignments ($\theta_d = 0^o$) of the 5CB molecule with the silver metal layer. **a** Different degrees of ordering; **b** sensitivity for various concentrations of the biological agent (Δn)
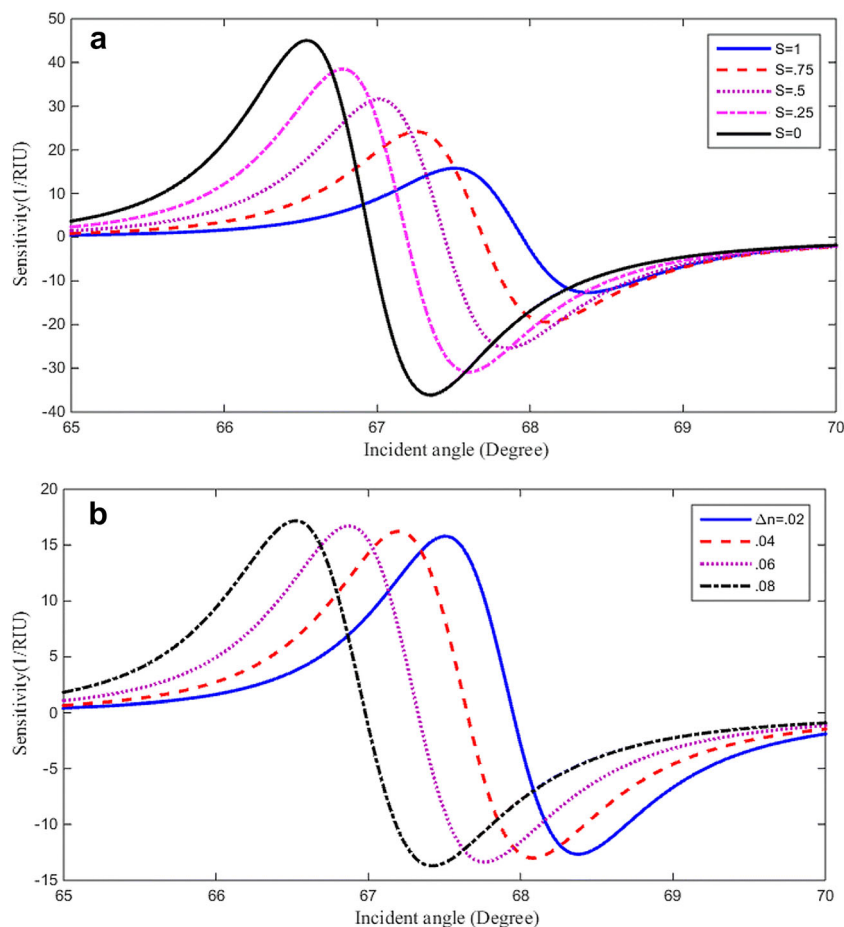
Results and Discussion

The thickness of gold and silver layers for the proposed LC-SPR biosensor is optimized for enhancing its sensing performance. As shown in Fig. 2, the gold (silver) layer thickness is optimized for achieving maximum sensitivity.

It was found that minimum reflectance and maximum sensitivity were obtained for 54 (57) nm gold (silver) thickness. After optimizing the metal thickness of the proposed LC-SPR

Table 1 Comparison of resonance angle, minimum reflection, FWHM, sensitivity, resonance shift angle, detection accuracy, and quality factor of LC-SPR biosensors in homeotropic alignments

| ($\theta_d = 0^o$)	θ_{res}(Deg.)	R_{min}	FWHM(Deg.)	$S\left(^o/_{RIU}\right)$	$\Delta\theta$(Deg.)	DA	QF$\left(^1/_{RIU}\right)$
(a) Au							
$S = 1$	70.98	0.1235	6.23	3.694	2.93	0.47	26.94
$S = 0.5$	65.41	0.0788	4.03	10.98	8.50	2.11	155.91
$S = 0$	61.64	0.0610	2.96	16.47	12.27	4.14	323.28
$\Delta n = 0.02$	73.69	0.1585	5.11	3.694	2.70	0.52	41.27
$\Delta n = 0.08$	72.58	0.1428	5.20	4.192	1.91	0.36	45.85
(b) Ag							
$S = 1$	64.76	0.1099	1.64	15.78	3.48	2.12	551.53
$S = 0.5$	61.33	0.0979	1.15	31.64	6.91	6.00	1577.04
$S = 0$	58.61	0.0910	0.90	45.02	9.63	10.70	2867.27
$\Delta n = 0.02$	67.95	0.1264	1.49	15.78	3.19	2.14	607.05
$\Delta n = 0.08$	66.98	0.1207	1.44	17.17	2.22	1.54	683.46

Table 2 Comparison of resonance angle, minimum reflection, FWHM, sensitivity, resonance shift angle, detection accuracy and quality factor of LC-SPR biosensors in homogeneous alignments

$(\theta_d = 90^o)$	$\theta_{res}(Deg.)$	R_{min}	FWHM(Deg.)	$S\left(^o/_{RIU}\right)$	$\Delta\theta(Deg.)$	DA	QF $\left(1/_{RIU}\right)$
(a) Au							
$S = 1$	59.87	0.0548	2.30	19.52	14.04	6.10	486.47
$S = 0.5$	60.78	0.0579	2.58	17.91	13.13	5.08	397.90
$S = 0$	61.64	0.0610	2.95	16.47	12.27	4.16	320.02
$\Delta n = 0.02$	60.93	0.0584	2.44	30.92	11.66	4.78	726.36
$\Delta n = 0.08$	64.58	0.0743	3.04	26.48	6.27	2.06	499.28
(b) Ag							
$S = 1$	57.51	0.0888	0.72	51.26	10.73	14.90	4080.86
$S = 0.5$	58.13	0.0899	0.80	47.71	10.11	12.63	3418.42
$S = 0$	58.61	0.0910	0.89	45.02	9.63	10.82	2899.49
$\Delta n = 0.02$	58.40	0.0905	0.76	74.53	9.11	11.98	5621.13
$\Delta n = 0.08$	61.39	0.0981	0.93	65.13	5.11	5.49	4014.24

sensor, curves were plotted for various conditions. The laser light was TM-polarized with an angle of incidence at the glass/metal interface. A variation in the structure at the LC/agents boundary was produced by binding of a chemical or biological agent. As a result, biomolecular interactions were significantly amplified in the average molecular alignment of the LC film. Therefore, for determining resonance angle, the angle of incidence was adjusted to achieve the minimum reflected

Fig. 7 reflection curves in homogeneous alignments ($\theta_d = 90^o$) of the 5CB molecule with the gold metal layer. **a** Different degrees of ordering; **b** reflection spectrums for various concentrations of the biological agent (Δn) in $S = 1$
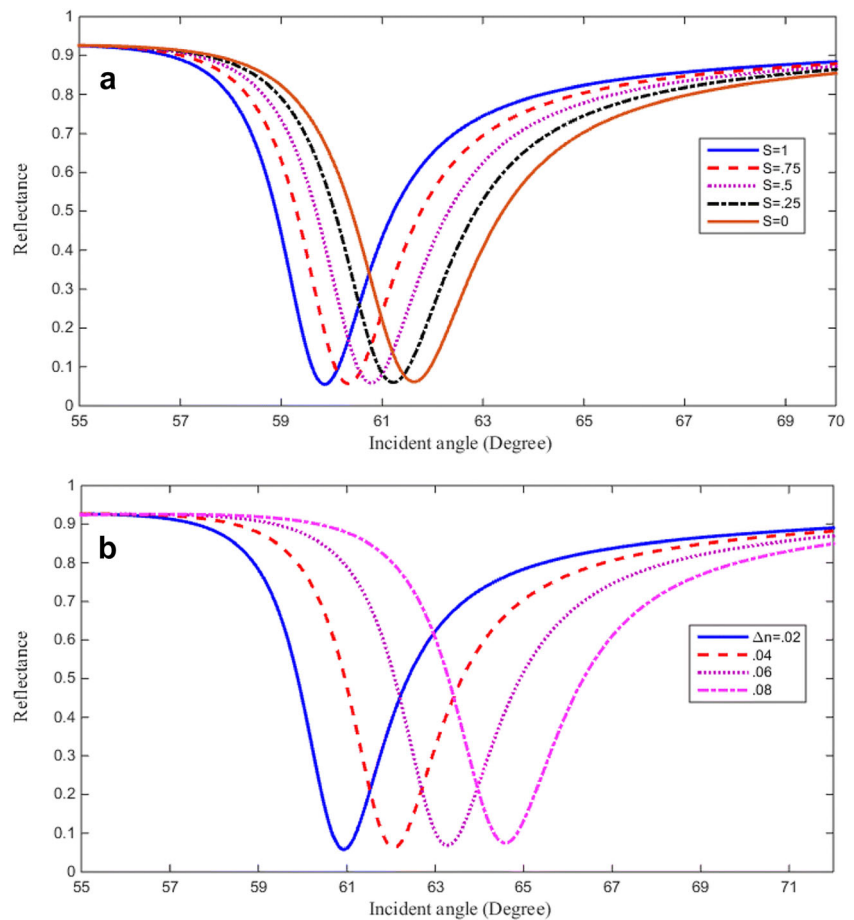
intensity. In experimental works, the anchoring layer may be weakened by exposing the ultraviolet radiation and by treating the metal surface with the low concentration solution of cetyltrimethylammonium bromide (CTAB), respectively.

In this work, the 5CB liquid crystal was used at room temperature ($T = 295.5^{\circ}$K) with extraordinary and ordinary refractive indices of $n_e = 1.7123$ and $n_o = 1.5305$ respectively at 633 nm [25, 26].

In the first case, molecules were normally aligned on the metal/LC interface (homeotropically aligned) and the director zenithal angle is $\theta = 0^o$. Figure 3 a and b shows reflection spectrums at different degrees of ordering and various concentrations of biological agent (Δn) for the gold metal layer. In Fig. 3, it was shown that the angle of resonance was shifted to the left when the order parameter was reduced and the concentration was increased.

Figures 4 a and b shows sensitivity at different degrees of ordering and various concentrations of biological agents (Δn) for gold as a metal layer. As shown in Fig. 4, the maximum sensitivity is increased and moved to the left by the decreasing order parameter and increasing birefringence. Figure 4 b depicts that the biosensor is sensitive for low concentration.

The results of the silver layer are given and compared with those of gold layer. Figure 5 illustrates reflectance and resonance angles with respect to different degrees of ordering and various concentrations of biological agents (Δn) when the silver layer is used in biosensor. As shown in Fig. 5, the angle of resonance is shifted to the left when the order parameter is reduced and the birefringence is increased. Also, the comparison of the results given in Fig. 5, with those of Fig. 3, indicate that the resonance occurs in small angles and SPR curves are narrowed with respect to gold-based structure.

Figures 6 a and b depicts the sensitivity of the silver-based structure. As depicted in Fig. 6a, the maximum sensitivity is enhanced and is shifted to the left by reducing the order parameter. As shown in Fig. 6b, by reducing concentration, the sensitivity increase is slightly more than that of the gold-based biosensor.

Resonance angle (θ_{res}), minimum reflectance (R_{min}), FWHM, sensitivity (S), detection accuracy (DA), and quality factor (QF) are calculated using Eqs. (12–14) for the LC-SPR biosensor in homeotropic alignments. For comparing gold- and silver-based structures, the results for some cases are tabulated in Tables 1 and 2.

Fig. 8 Sensitivity in homogeneous alignments ($\theta_d = 90^o$) of the 5CB molecule with the gold metal layer. **a** Different degrees of ordering; **b** sensitivity for various concentrations of the biological agent (Δn) in $S = 1$
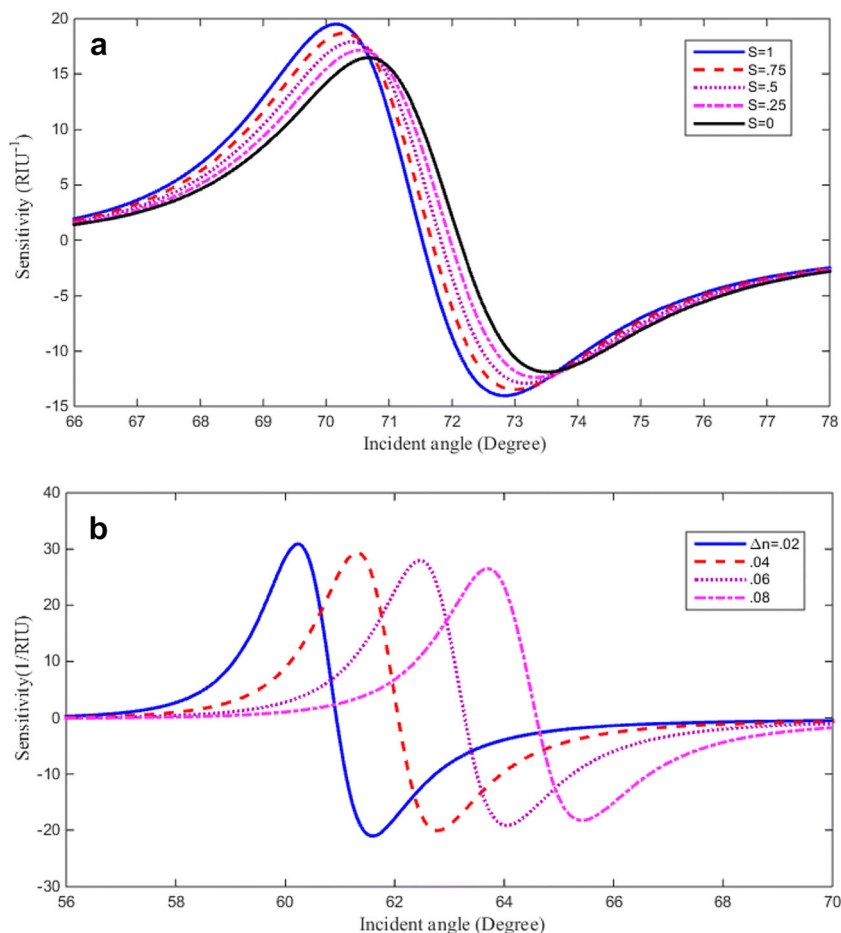
As given in Table 1, maximum sensitivity, detection accuracy, quality factor, and other performance parameters of the proposed LC-SPR biosensor were achieved for $S = 0$ situation. Performance parameters of the silver-based structure were higher than those of the gold-based structure. A smaller DA value can be compensated because our results show a high-quality factor and good sensitivity which are useful for detecting biological analytes.

In the second case, it was assumed that molecules were parallel to metal/LC interface (homogeneously aligned) and the director zenithal angle was $\theta = 90^{\circ}$. Figure 7 a and b shows reflection spectrums at different ordering degrees and various concentrations of biological agents for gold as the metal layer. These figures indicated that the resonance angle is shifted to the right when the order parameter and concentration are reduced.

Figure 8 a and b depicts sensitivity at different ordering degrees and various concentrations of biological agents for gold in homogeneous alignments. As depicted in these figures, maximum sensitivity decreases and resonance angles are shifted to the right by reducing order parameters and increasing birefringences, respectively.

Figures 9 and 10 depict the results for the silver layer in the homogeneous alignment and compare them with the previous results. Figure 9 shows the reflectance and resonance angle with respect from the different ordering degrees and various concentrations of biological agents (Δn) for the silver layer case used in the biosensor. As demonstrated in Fig. 9, the resonance angle is shifted to the right when the order parameter is reduced and the birefringence is increased. Moreover, comparing the results of Fig. 9 with those of Fig. 7 which indicates that resonance angles occur in small angles and SPR curves are narrowed with respect to the gold-based structure.

Figures 10 a and b shows sensitivity for homogeneous alignment in the silver-based structure. As given in Fig. 10a, the maximum sensitivity is reduced and is shifted to the right as the order parameter decreases. Figure 10 b indicates that, as a result of a decreased concentration, the sensitivity increase in the silver-based structure is slightly more than that of the gold-based biosensor.

As shown in Table 2, maximum sensitivity, detection accuracy, quality factor, and other performance parameters of the LC-SPR proposed biosensor were obtained for the $S = 1$

Fig. 9 Reflection curves in homogeneous alignment ($\theta_d = 90^{\circ}$) of the 5CB molecule with the silver metal layer. **a** Different degrees of ordering; **b** reflection spectrums for various concentration of biological agent (Δn) in $S = 1$
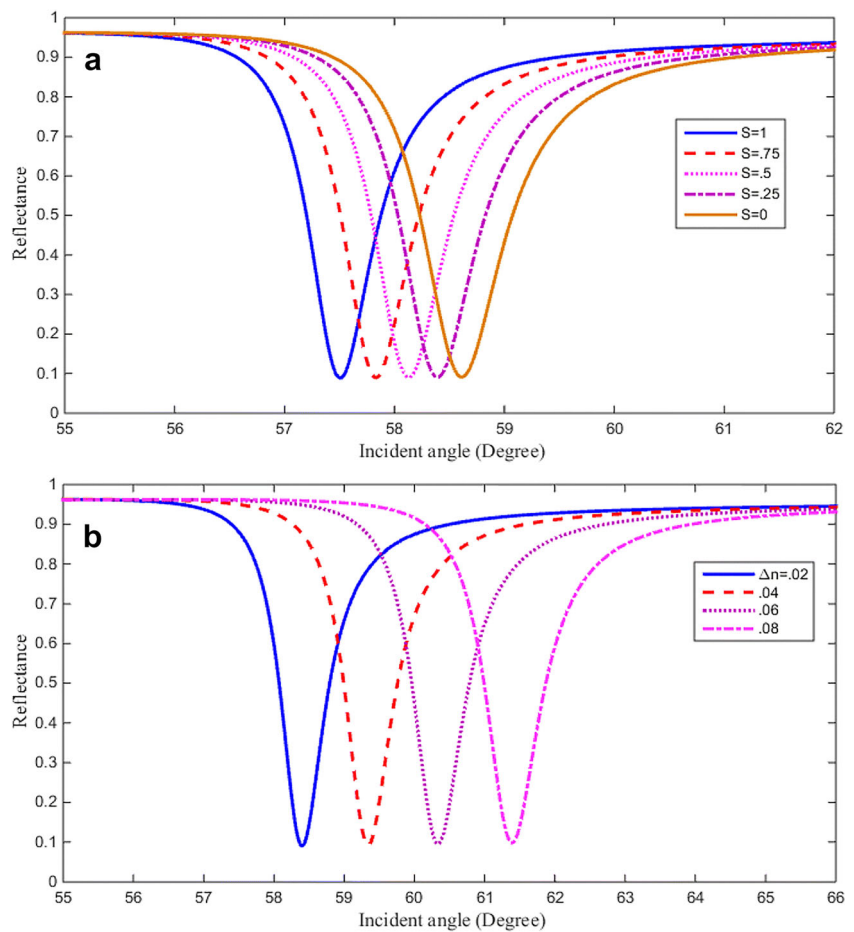
Fig. 10 Sensitivity in homogeneous alignments ($\theta_d = 90^o$) of the 5CB molecule at room temperature ($T = 22.5$ °C) with silver. **a** Different degrees of ordering; **b** sensitivity for various concentrations of the biological agent (Δn)
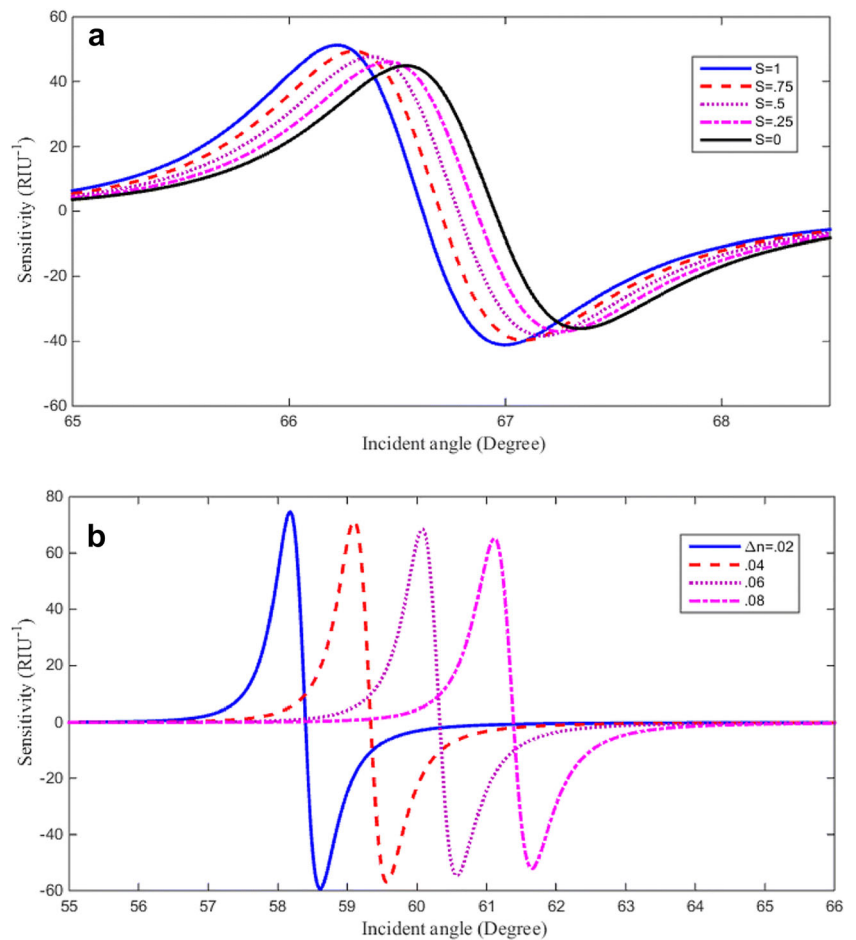
situation. It was found that performance parameters of silver-based structure and homogeneous alignments were higher than those of the gold-based structure.

Conclusion

Thanks to using an optical transduction mechanism, the proposed LC-SPR biosensor can efficiently sense analytes by detecting the alignment of liquid crystal. The results indicated significant the quality factor and sensitivity for the proposed sensor. Moreover, the investigations revealed that after adding, analytes and birefringences of the liquid crystal changes. Consequently, performance parameters were enhanced. Maximum performance parameters of the proposed LC-SPR biosensor were obtained for $S = 0$ and homogenous alignments situations. Furthermore, the results indicated that performance parameters of the silver-based structure were higher than those of the gold-based structure. Hence, as a direction for further research and development, the proposed biosensor can be used for detecting biological agents with a high degree of accuracy and quality.

References

1. Carlton RJ, Hunter JT, Miller DS, Abbasi R, Mushenheim PC, Tan LN, Abbott NL (2013) Chemical and biological sensing using liquid crystals. Liquid crystals reviews 1(1): 29–51
2. Niu X, Zhong Y, Chen R, Wang F, Luo D (2017) Highly sensitive and selective liquid crystal optical sensor for detection of ammonia. Opt Express 25(12):13549–13556
3. Reyes CG, Sharma ALagerwall JP (2016) Non-electronic gas sensors from electrospun mats of liquid crystal core fibres for detecting volatile organic compounds at room temperature. Liq Cryst 43(13–15):1986–2001
4. Rashiditabar R, Nozhat N, Zare MS (2018) Tunable plasmonic absorber based on TiN-nanosphere liquid crystal hybrid in visible and near-infrared regions. Plasmonics. 13(6): 1853–1859
5. Vahedi E, Tajalli H, Gilani AG, Parka J, Milani HN (2010) Electro-optical Kerr effect in the isotropic phase of the two antiferroelectric liquid crystal mixtures. Phase Transit 83(6):432–439
6. Yang S, Wu C, Tan H et al (2012) Label-free liquid crystal biosensor based on specific oligonucleotide probes for heavy metal ions. Anal Chem 85(1):14–18
7. Yoon SH, Gupta KC, Borah JS, Park SY, Kim YK, Lee JH, Kang IK (2014) Folate ligand anchored liquid crystal microdroplets emulsion for in vitro detection of KB cancer cells. Langmuir. 30(35): 10668–10677

8. Deng S, Jiang Q, Zhang T, Xiong X, Chen P (2015) Liquid crystal biosensor based on Cd2+ inducing the bending of PS-oligo for the detection of cadmium. Health. 7(08):986

9. Abuabed ASA (2017) Study of the effect of nematic order degradation in liquid crystal-based surface plasmon resonance sensors. Photonics. 4(2):24

10. Niu X, Luo D, Chen R, Wang F, Sun X, Dai H (2016) Optical biosensor based on liquid crystal droplets for detection of cholic acid. Opt Commun 381:286–291

11. Popov P, Honaker LW, Kooijman EE, Mann EK, Jákli AI (2016) A liquid crystal biosensor for specific detection of antigens. Sensing and bio-sensing research 8:31–35

12. Khan M, Park SY (2015) Liquid crystal-based glucose biosensor functionalized with mixed PAA and QP4VP brushes. Biosens Bioelectron 68:404–412

13. Otto A (1968) Excitation of nonradiative surface plasma waves in silver by the method of frustrated total reflection. Zeitschrift für Physik A Hadrons and Nuclei 216(4):398–410

14. Alharbi R, Irannejad M, Yavuz M (2017) Gold-graphene core-shell nanostructure surface plasmon sensors. Plasmonics. 12(3):783–794

15. Liu Y, Liu X, Chen S, Liu Q, Peng W (2016) Investigation of a capillary-based surface plasmon resonance sensor for biosensing. J Lightwave Technol 34(17):4036–4042

16. Hodnik VAnderluh G (2009) Toxin detection by surface plasmon resonance. Sensors. 9(3):1339–1354

17. Konopsky VN, Alieva EV (2010) A biosensor based on photonic crystal surface waves with an independent registration of the liquid refractive index. Biosens Bioelectron 25(5):1212–1216

18. Rifat AA, Ahmed R, Yetisen AK, Butt H, Sabouri A, Mahdiraji GA, Yun SH, Adikan FRM (2017) Photonic crystal fiber based plasmonic sensors. Sensors Actuators B Chem 243:311–325

19. Ruan L, Yang F, Sambles JR (2009) Otto-coupled surface plasmons in a liquid crystal cell. Appl Phys Lett 95(17):171102

20. Lu M, Zhang X, Liang Y, Li L, Masson JF, Peng W (2016) Liquid crystal filled surface plasmon resonance thermometer. Opt Express 24(10):10904–10911

21. Kieser B, Pauluth D, Gauglitz G (2001) Nematic liquid crystals as sensitive layers for surface plasmon resonance sensors. Anal Chim Acta 434(2):231–237

22. Wang G, Wang C, Yang R, Liu W, Sun S (2017) A sensitive and stable surface plasmon resonance sensor based on monolayer protected silver film. Sensors. 17(12):2777

23. Xu H, Wu L, Dai X, Gao Y, Xiang Y (2016) An ultra-high sensitivity surface plasmon resonance sensor based on graphene-aluminum-graphene sandwich-like structure. J Appl Phys 120(5):053101

24. Prost J (1995) The physics of liquid crystals. Vol. 83. : Oxford university press

25. Khoo I-C (2007) Liquid crystals. Vol. 64. : John Wiley & Sons

26. Abu-Abed AS (2009) Optical waves in partially ordered anisotropic media. Opt Express 17(3):1646–1651

27. Popov P, Mann EK, Jakli A (2017) Thermotropic liquid crystal films for biosensors and beyond. J Mater Chem B 5(26):5061–5078

28. Popov P, Mann EK, Jakli A (2014) Accurate optical detection of amphiphiles at liquid-crystal–water interfaces. Physical review applied 1:034003

29. Pal S, Verma A, Raikwar S et al (2018) Detection of DNA hybridization using graphene-coated black phosphorus surface plasmon resonance sensor. Applied Physics A 124:1–11